Organic & Biomolecular Chemistry

Accepted Manuscript

ROYAL SOCIETY OF CHEMISTRY

www.rsc.org/obc

Cite this: DOI: 10.1039/c0xx00000x

www.rsc.org/xxxxxx

ARTICLE TYPE

Reversal of H-bonding Direction by N-Sulfonation: A Case Study With a Synthetic Reverse-Turn Peptide Motif‡

Kuruppanthara N. Vijayadas,[a] Amol S. Kotmale,[b] Shridhar H. Thorat,[c] Rajesh G. Gonnade,[c] Roshna V. Nair,[a, d] Pattuparambil R. Rajamohanan,[b] and Gangadhar J. Sanjayan*[a]

Received (in XXX, XXX) Xth XXXXXXXXX 20XX, Accepted Xth XXXXXXXXX 20XX

DOI: 10.1039/b000000x

This communication depicts an intriguing example of hydrogen-bonding reversal upon introduction of sulfonamide linkage at the N-terminus of a synthetic reverse-turn peptide motif. The ready availability of two sulfonyl oxygen atoms, as hydrogen-bonding acceptors, combined with the inherent twisted conformation of sulfonamides are seen to act as switches that engage/disengage the hydrogen-bond at the sticky ends/termini.

Introduction

Hydrogen-bonding, one of the prominent non-covalent interactions, plays a significant role in rigidifying the conformation of biopolymers – especially peptides and proteins. The highly directional nature of H-bonding is the primary cause for the precise folding phenomenon in various protein secondary structures like reverse turns, helices, β-sheets, *etc*. Reverse turns are the smallest secondary structural units with wide range of functions in biological systems and their mimics are one of the most preferred motifs for the development of peptide derived drugs.[1] Introduction of sulfonamide functionality into peptides provides a solution for the limited usage of proteolytically unstable peptide drugs.[2] Moreover, the modified peptido-sulfonamide linkages can act as an interesting structural motifs for peptidomimetics due to their immense bio-active properties.[3] The key feature of sulfonamide, an efficient surrogate of carboxamide linkage, is the presence of two oxygen atoms that enhances the hydrogen-bonding possibilities. In addition, the limited rotation barrier about the S-N bond, along with the dihedral disparity of ~90° (compared to 180° of carboxamides) renders twists to peptide chains.[3]

In this regard, the use of orthanilic acid has earned special attention due to its intrinsic feature of inducing reverse turn formation as well as structural rigidification in peptides.[4,5] Our earlier studies on orthanilic acid (^{S}Ant) and ^{L}proline (Pro)-derived dipeptides led to the discovery of reverse turn motifs featuring strong C-9 or C-11 *inter*-residual H-bonding in the sequence order of β/α and α/β, respectively.[4,5]

In earlier investigations, it was found that when ^{S}Ant was conjoined with Pro - a conformationally constrained amino acid, it preserved the *pseudo*-β-turn assembly, by assuming the highly deviated C-S-N-C dihedral angle 'ω' = 163° ('ω' ~ 160° for carboxamide analogues).[4] This instance demonstrated that the fundamental torsional preference of ^{S}Ant (sulfonamide bond) could be dramatically modulated by the influence of adjoining residues. Extending the torsional restraints by addition of another Pro unit to the N-terminus of the ^{S}Ant-Pro turn motif also retained the similar conformational features, as seen in peptide **1**.

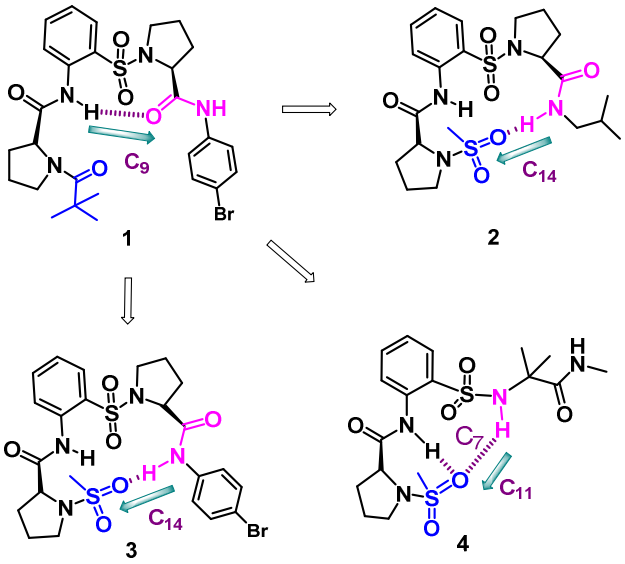

Fig. 1: Molecular structures of *Xaa*-^{S}Ant-*Yaa* turn motifs with the observed hydrogen-bonding patterns. *Note*: The H-bonding sites and their orientation have been highlighted.

Intriguingly, substitution of the N-terminus carboxamide in **1** by sulfonamide, as in **2**-**4**, resulted in dramatic conformational change which could be clearly seen from their crystal structures (Fig. 2). Sulfonamide analogs **2** and **3** feature a terminal C-14 hydrogen-bonding network with d(N-H···O) = 2.4Å. The hydrogen-bonding interactions were seen to be involving oxygen of SO of the i^{th} residue and the NH of the $(i + 4)^{th}$ residue, in the backward direction (5←1), akin to typical α-turns (5 residues in C-13 turn).[6] And in **4**, wherein the C-terminal Pro was replaced with constraint amino acid 2-aminoisobutyric acid (Aib),[7] a weak C-7 hydrogen-bonding is also observed, in addition to a C-11 hydrogen-bonding.

Results and Discussion

Synthesis

Compounds **1-7**, required for the present study, were synthesized using multi-step synthetic strategies, as depicted in schemes 1-3 (ESI, page S3-S5).

Conformational Analysis

Solid-state structural studies

From the previous studies, it was noted that both the dihedral constraints 'ω' of sulfonamide bond and 'θ' of ^{S}Ant play crucial role in the formation and stabilization of ^{S}Ant-Pro C-9 hydrogen-bonding.[4] Torsion angle 'ω' in tripeptide **1** also adopted the unusual value of 152°[8] as it featured the presence of ^{S}Ant-Pro C-9 turn with hydrogen-bonding distance [d(N-H···O): 2.2Å] (Table 1, *vide infra*).

It was noted that the ^{S}Ant-Pro motif, which was devoid of a pseudo β-turn (C-9 turn) in **2** and **3**, showed the C-S-N-C dihedral angle 'ω' close to a value of 66°, which is of a typical sulfonamide bond. The three-dimensional architecture of the tripeptide with characteristic C-14 hydrogen-bonding was well evidenced from solid-state single crystal X-ray diffraction studies of **2** and **3**. Thus, the sulfonamide-to-carboxamide modification at the N-termini completely abolished the C-9 conformation observed in **1**, indicating the significance of the twisted sulfonamide bond in bringing the hydrogen-bonding sites into proximity and thereby, altering the hydrogen-bonding patterns as observed in the carboxamide analog **1**.

In order to explore the role of torsional requisites causing the formation of this 5-residue turn featuring a planar aromatic residue, we carried out further structural alterations within the tripeptide sequence, including the replacement of terminal pro residues with another constrained amino acid 2-aminoisobutyric acid (Aib) - an unnatural α-aminoacid with unique preferences of dihedral angles to induce folding in peptides.[7] The significance of the dihedral angle constraints and their structural implications were thereby expounded. Substitution effects within the turn motif resulted in deleterious effect on the C-14 hydrogen-bonding pattern, when the N- and C-terminal prolines were swapped with Aib. This modification also revealed the involvement of an additional 'NH' as a hydrogen-bond donor unlike to that of proline. In the tripeptide **4** (Fig 2), the Aib at the N-terminus showed the involvement of Aib 'NH' in an 11-membered hydrogen-bonding with proline 'SO' in the backward direction (4←1) [d(N-H···O): 2.3Å]. The turn system also featured a weak 7-membered H-bonding between the terminal sulfonyl 'O' and ^{S}Ant 'NH', in the backward direction (3←1) [d(N-H···O): 3.0Å], similar to typical γ-turns (3 residue C-7 turn).[9]

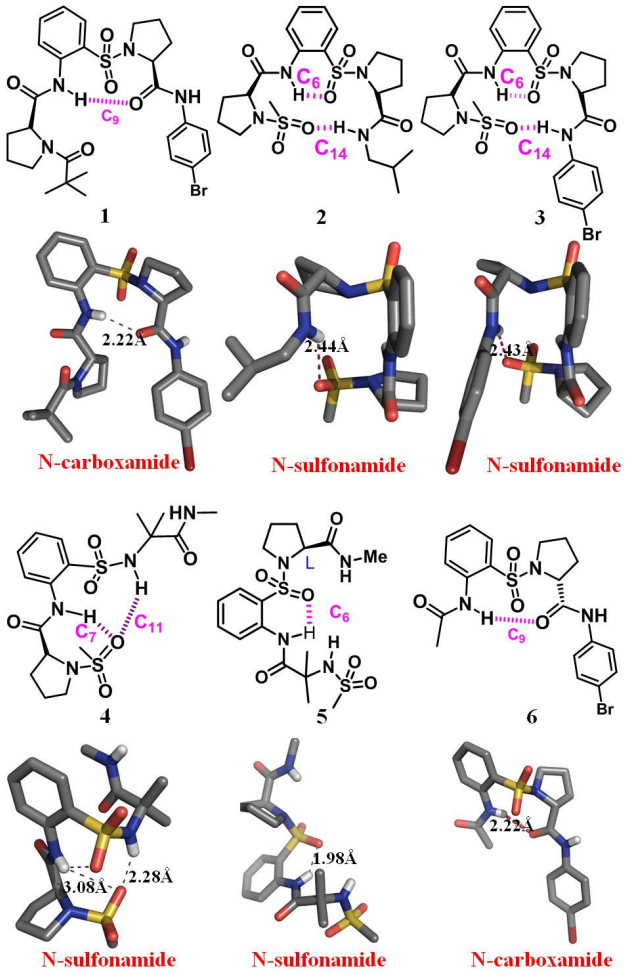

Fig. 2: Molecular structures of **1-6**, along with their crystal structures.

Table 1. Table showing the crystal data analysis of peptides **1-7**

Compound No.	Torsional Parameters (deg.)									Type of inter-residual H-bonding[a]	Torsion Angle C=O···H-N (deg.)	H-bonding Distance d (NH···O) (Å)
	Xaa		^{S}Ant			*Yaa*		CSNC dihedral angle for sulfonamide bond				
	φ	ψ	φ	θ	ψ	φ	ψ	ω1	ω2			
1	-67.00	146.81	-127.75	8.19	-66.93	-112.56	**168.11**	**155.17**	-	C-9	76.90	2.216
2	-86.86	-31.16	-178.38	-1.01	-71.75	-104.28	-19.44	-68.72	66.55	C-14	163.29	2.478
3	-118.80	11.82	167.80	1.25	-69.47	-95.56	-34.47	-58.74	58.78	C-14	-121.60	2.436
4	-107.89	6.11	-145.57	-0.51	69.16	-73.91	**120.54**	-74.22	61.71	Weak C-7 & C-11	-127.91 -92.91	3.030 2.292
5	-67.21	-45.70	166.28	-9.41	-91.78	-116.43	-10.20	-88.43	-74.75	-	-	-
6	-	-	-158.56	-0.69	61.57	86.66	**-163.12**	**-163.29**	-	C-9	-161.98	2.210
7	-	-	148.56	6.17	-68.56	-72.75	**147.82**	**155.86**	-	C-9	120.93	2.132

[a]*inter-residual* hydrogen-bonding.

The substitution of N-terminus Pro with Aib abolished the C-9 hydrogen-bonding too, a prominent feature of ^{S}Ant-Pro turn systems and the resultant crystal structure, instead, showed the C-6 hydrogen-bonding of ^{S}Ant in **5** (Fig. 2). The absence of 9-membered hydrogen-bonding was due to the presence of dihedral constraints, as discussed earlier. Replacement of L-Pro of ^{S}Ant-Pro turn motif with D-Pro and *NMe*-Aib resulted in the persistance of C-9 hydrogen-bonding networks in **6** (Fig. 2) and **7** (ESI S72). In those cases, the 'ω' remain 163° and 155° for **6** and **7**, respectively. This experimentation suggested that the N-methyl constraints of Pro and *NMe*-Aib residue have major roles in maintaining the large value for C-S-N-C dihedral angle 'ω' for sulfonamide bond.[10] The absence of ^{S}Ant-Pro 9-membered hydrogen-bonding in **2**-**4** is mainly due to the dihedral constraints offered by N-terminal Pro/Aib residues.

The conformational changes that occur upon backbone modification[11], governed by their ϕ and ψ values, are summarized in table-1 (*vide supra*). From the table, it is apparent that the sulfonamide group has provided the prolific use of its acceptor sulfonyl oxygens for hydrogen-bonding interactions, although weak, and induce folding owing to its inherent twisted geometry.

Solution-state NMR studies

The solution-state behavior of **1** was also evaluated from 2D NOESY studies (ESI S52-S53), which supported the presence of C-9 H-bonding pattern. NMR DMSO-d_6 titration (δNH1 = 0.08ppm & δNH2 = 0.33ppm) and variable temperature experiments (δNH1 = 0.07ppm; $\Delta\delta/\Delta T$ = -1.27ppbK^{-1} & δNH2 = 0.23ppm; $\Delta\delta/\Delta T$ = -4.18ppbK^{-1}) in $CDCl_3$ (ESI S61 & S64), validated the strength of the hydrogen-bonding interaction.

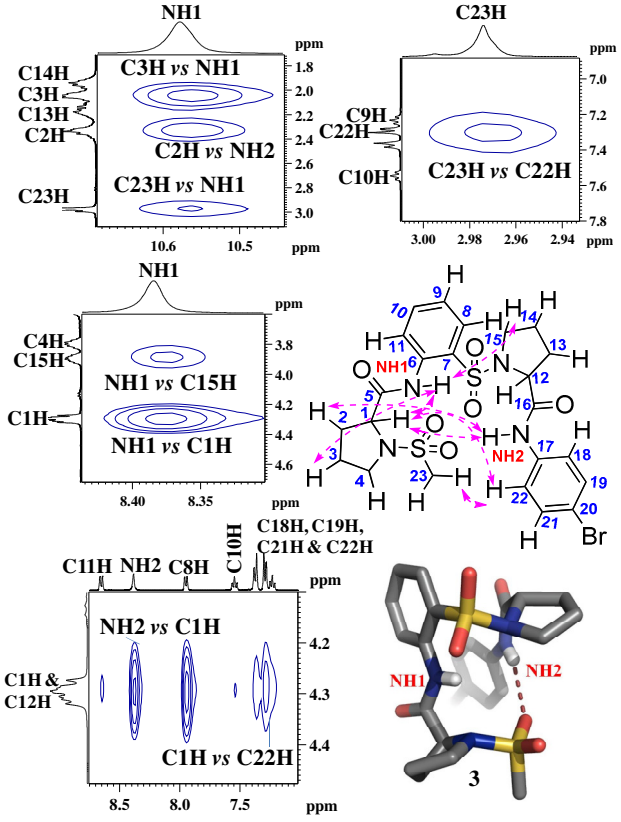

Fig. 3: Figure showing the selected 2D NOESY extracts of **3.**

Also, the solution-state NMR 2D NOESY studies of **3** confirmed its C-14 hydrogen-bonded arrangement through the diagnostic NOEs like NH2 *vs* C1H, C1H *vs* C18H, C23H *vs* C22H & NH1 *vs* C15H (Fig. 3 and ESI, S49-S50). The nature of hydrogen-bonding interactions (intra *vs* inter) were studied by DMSO-d_6 titration (Fig. 4B) and variable temperature (Fig. 4C) studies in $CDCl_3$, where both the NHs showed negligible chemical shift (δNH ≤ 0.13ppm; ESI, S60 and S64), suggestive of robust intramolecular C-14 hydrogen-bonding.

Thus, the sulfonamide-to-carboxamide modification at the N-termini completely abolished the C-9 conformation observed in **1**, indicating the significance of the twisted sulfonamide bond in bringing the hydrogen-bonding sites into proximity and thereby, altering the hydrogen-bonding patterns as observed in the carboxamide analog **1**.

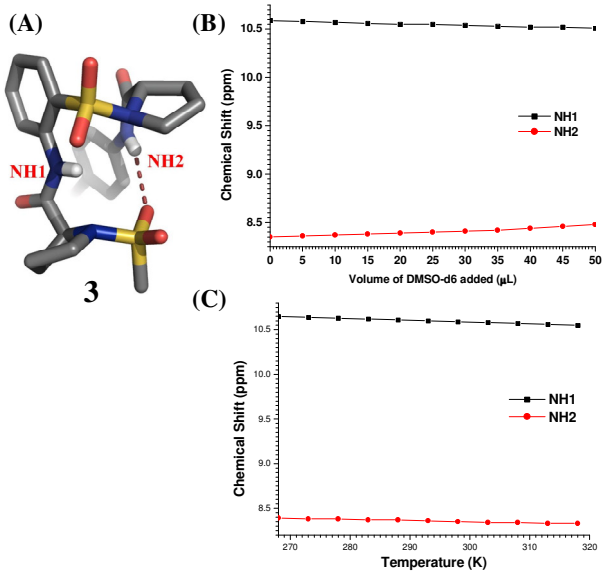

Fig. 4: PyMol rendered crystal structure (A), stacked plots of NMR DMSO-d_6 titration studies (B) and variable temperature studies (C) of **3** (400 MHz, 5 mmol, $CDCl_3$)**.**

In order to explore the role of torsional requisites causing the formation of this 5-residue turn featuring a planar aromatic residue, we carried out further structural alterations within the tripeptide sequence, including the replacement of terminal pro residues with another constrained amino acid 2-aminoisobutyric acid (Aib) - an unnatural α-aminoacid with unique preferences of dihedral angles to induce folding in peptides.[7] The significance of the dihedral angle constraints and their structural implications were thereby expounded. Substitution effects within the turn motif resulted in deleterious effect on the C-14 hydrogen-bonding pattern, when the N- and C-terminal prolines were swapped with Aib. This modification also revealed the involvement of an additional 'NH' as a hydrogen-bond donor unlike to that of proline. In the tripeptide **4** (Fig 2), the Aib at the N-terminus showed the involvement of Aib 'NH' in an 11-membered hydrogen-bonding with proline 'SO' in the backward direction (4←1) [d(N-H···O): 2.3Å]. The turn system also featured a weak 7-membered H-bonding between the terminal sulfonyl 'O' and ^{S}Ant 'NH', in the backward direction (3←1) [d(N-H···O): 3.0Å], similar to typical γ-turns (3 residue C-7 turn).[9] This was clearly revealed

in their solution-state 2D NMR studies as well (ESI S58-S59), solvent titration (ESI S63) and variable temperature studies (ESI S66). The solid-state behaviour of **5** was well reflected in the solution-state 2D NOESY studies (ESI S55-S56). The presence of *intra*-molecular hydrogen-bonding was vindicated from the negligible chemical shifts observed from DMSO-d_6 titration studies (δNH1 = 0.33ppm, δNH2 = 0.1 ppm & δNH3 = 0.23ppm) and variable temperature NMR studies carried out in $CDCl_3$ (δNH1 = 0.33ppm; $\Delta\delta/\Delta T$ = -6ppbK^{-1}, δNH2 = 0.07ppm; $\Delta\delta/\Delta T$ = -1.27ppbK^{-1}, δNH3 = 0.21ppm; $\Delta\delta/\Delta T$ = -3.82ppbK^{-1}) (ESI S62 & S67).

Conclusions

In summary, the work presented herein illustrates the reversal of hydrogen-bonding orientation at the termini, when a N-carboxamide moeity is swapped with N-sulfonamide. The three-residue folded peptides mesyl-Pro-^{S}Ant-Pro **2** and **3** exhibited an unusual C-14 membered hydrogen-bonding pattern, unlike that of Piv-Pro-^{S}Ant-Pro **1** that adopts C-9 turn. The mutation of Pro to Aib at both termini validated the essentiality of Pro unit in the formation of C-14 hydrogen-bond. The different folding patterns are dependent on the terminal aminoacid residues (*i* and *i*+2) and presence of sulfonamide bond between the residues as evidenced from single crystal analyses[12] and NMR studies. This work illustrates the implications of the conformational features of peptides when the N-terminus is swapped with sulfonamide group with its distinctive geometrical and hydrogen-bonding preferences - starkingly different when compared to its carboxamide counterpart.

Acknowledgement

KNV, RVN & ASK thank CSIR (New Delhi) for research fellowships. This work was funded by CSIR Biodiversity network programme (BSC-0120).

Experimental procedures

Crystal X-ray Crystallographic Studies:

Crystallographic Data for the compounds **1**, **2**, **3**, **4** and **5** were collected on SMART APEX-II CCD using Mo-Kα radiation (λ = 0.7107 Å) to a maximum θ range of 25.00°. Crystal to detector distance 5.00 cm, 512 x 512 pixels / frame, Oscillation / frame -0.5º, maximum detector swing angle = –30.0º, beam center = (260.2, 252.5), in plane spot width = 1.24, SAINT integration with different exposure time per frame and SADABS correction applied. All the structures were solved by direct methods using SHELXTL. All the data were corrected for Lorentzian, polarisation and absorption effects. SHELX-97 (ShelxTL) was used for structure solution and full matrix least squares refinement on F^2. Hydrogen atoms were included in the refinement as per the riding model.

Crystal data for 1

Single crystals of **1** were grown by slow evaporation of the solution mixture of ethyl acetate and pet. ether. Colorless block crystal of size 0.49 x 0.42 x 0.31 mm^3, was used for data collection, Temperature = 296(2) K, Wave length = 0.71073 Å Quadrant data acquisition, F(000) = 1256, θ range = 1.76° to 28.29°, completeness to θ is 100 %, Goodness-of-fit on F2 = 1.067, $C_{27}H_{33}BrN_4O_5S$, M = 605.54. Crystals belong to Orthorhombic, space group P212121, a = 6.7186(2) , b = 15.8096(5), c = 26.5176(7) Å, α = β = γ = 90º, V = 2816.66(14) $Å^3$, Z = 4, Dc = 1.428 g/cc, μ (Mo–Kα) = 1.577 mm-1, 6952 total reflections, 4854 unique reflections, R value 0.0698, wR2 = 0.1124.

Crystal data for 2

Single crystals of **2** were grown by slow evaporation of the solution mixture of ethylacetate and pet.ether. Colorless needle crystal of size 0.64 x 0.19 x 0.13 mm^3, was used for data collection, Temperature = 297(2)K, Wave length = 0.71073 Å Quadrant data acquisition, Total scans = 4, F(000) = 1064, θ range = 2.19° to 25.49°, completeness to θ of 24.99 º is 100 %, Goodness-of-fit on F2 = 1.018, $C_{21}H_{32}N_4O_6S_2$, M = 500.63. Crystals belong to Monoclinic, space group C2, a = 18.6244(11), b = 8.4267(4), c = 16.0611(8) Å, α = 90, β = 93.118(5), γ = 90, 2516.9(2) Å3, Z = 4, Dc = 1.321 g/cc, μ (Mo–Ka) = 0.254 mm-1, 4429 total reflections, 4052 unique [I>2s(I)], R value 0.0430, wR2 = 0.1171.

Crystal data for 3

Single crystals of **3** were grown by slow evaporation of the solution mixture of ethylacetate and pet.ether. Colorless needle crystal of size 0.65 x 0.33 x 0.29 mm^3, was used for data collection, Temperature = 296(2)K, Wave length = 0.71073 Å Quadrant data acquisition, F(000) = 616, θ range = 2.36° to 30.42°, completeness to θ is 95 %, Goodness-of-fit on F2 = 0.993, $C_{23}H_{27}BrN_4O_6S_2$, M = 599.53. Crystals belong to Monoclinic, space group P21, a = 8.1060(12) , b = 10.5928(16), c = 14.983(2) Å, α = 90, β = 96.273(8), γ = 90, V = 1278.8(3) $Å^3$, Z = 2, Dc = 1.557 g/cc, μ (Mo–Kα) = 1.817 mm-1, 7389 total reflections, 5331 unique reflections, R value 0.0355, wR2 = 0.0875.

Crystal data for 4

Single crystals of **4** were grown by slow evaporation of the solution mixture of ethylacetate and pet.ether. Colorless block crystal of size 0.50 x 0.45 x 0.35 mm^3, was used for data collection, Temperature = 296(2)K, Wave length = 0.71073 Å Quadrant data acquisition, F(000) = 944, θ range = 2.53 ° to 28.10°, completeness to θ is 100 %, Goodness-of-fit on F2 = 1.082, $C_{17}H_{26}N_4O_6S_2$, M = 446.54. Crystals belong to Orthorhombic, space group P212121, a = 9.5896(2), b = 14.7665(3), c = 14.7848(3) Å, α = β = γ = 90º, V = 2093.60(19) $Å^3$, Z = 4, Dc = 1.417 g/cc, μ (Mo–Kα) = 0.296 mm-1, 2902 total reflections, 2703 unique reflections, R value 0.0346, wR2 = 0.0908.

Crystal data for 5

Single crystals of **5** were grown by slow evaporation of the solution mixture of ethylacetate and pet.ether. Colorless plate crystal of size 0.47 x 0.31 x 0.05 mm^3, was used for data collection, Temperature = 297(2)K, Wave length = 0.71073 Å Quadrant data acquisition, F(000) = 472, θ range = 1.65° to 30°, completeness to θ is 87 %, Goodness-of-fit on F2 = 1.027, $C_{17}H_{26}N_4O_6S_2$, M = 446.54. Crystals belong to Monoclinic, space group P21, a = 7.7425(4), b = 10.0108(6), c = 13.8284(8) Å, α = 90, β = 102.033(3), γ = 90, V = 1048.27(10) $Å^3$, Z = 2, Dc = 1.415 g/cc, μ (Mo–Kα) = 0.296 mm-1, 5303 total reflections, 4805 uniq. reflections, R = 0.0317, wR2 = 0.0819

Crystal data for 6

Single crystals of **6** were grown by slow evaporation of the solution mixture of Dichloromethane and methanol. Colorless needle type crystal of approximate size 0.45 x 0.23 x 0.19 mm^3, was used for data collection, Temperature = 296(2) K, Wave length = 0.71073 Å, Quadrant data acquisition, Total scans = 4, F(000) = 952, θ range = 2.56° to 28.31°, Goodness-of-fit on F^2 = 0.988, $C_{19}H_{20}BrN_3O_4S$, M = 466.35. Crystals belong to Orthorhombic, space group P212121, a = 9.2942(10) Å, b = 13.9119(13) Å, c = 15.3096(17) Å, α = β = γ = 90°, V = 1979.5 (4) $Å^3$, Z = 4, Dc = 1.565 g/cc, μ (Mo–Kα) = 0.71073 mm-1, total reflections = 4865, 3065 unique reflections, R value 0.0432, wR_2 = 0.0926.

Crystal data for 7

Single crystals of **7** were grown by slow evaporation of the solution of methanol. Colorless block crystal of approximate size 0.66 x 0.27 x 0.14 mm^3, was used for data collection, Temperature = 297(2) K, Wave length = 0.227 Å, Quadrant data acquisition, F(000) = 348, θ range = 2.69 to 28°, completeness to θ of 28° is 99.3 %, Goodness-of-fit on F^2 = 1.059, $C_{14}H_{20}N_2O_5S$, M = 328.38. Crystals belong to Triclinic, space group P1, a = 7.1146(3) Å, b = 8.0387(3) Å, c = 15.0865(6) Å, α = 90.323(2), β = 100.054(2), γ = 109.252(2) , V = 800.21(6) $Å^3$, Z = 2, Dc = 1.363 g/cc, μ (Mo–Kα) = 0.227 mm-1, 3852 reflections collected, 3360 unique [I>2σ(I)], R value 0.0386, wR_2 = 0.1169.

Notes and references

[a]*Division of Organic Chemistry, National Chemical Laboratory, Dr. Homi Bhabha Road, Pune 411 008, India. Fax: +91-020-2590-2629; Tel+91-020-2590-2082; E-mail: gj.sanjayan@ncl.res.in Research Group: http://nclwebapps.ncl.res.in/gjsanjayan;*

[b]*Centre for Materials Characterisation, National Chemical Laboratory, Dr. Homi Bhabha Road, Pune 411 008, India.*

[c]*Central NMR Facility, National Chemical Laboratory, Dr. Homi Bhabha Road, Pune 411 008, India*

[d]*Current Address: Max-Planck-Institut für Polymerforschung, Ackermannweg 10, 55128 Mainz, Germany*

† Electronic Supplementary Information (ESI) available: ^1H, ^{13}C, DEPT-135 NMR, 2D study spectra, ESI mass spectra and theoretical study of new compounds are included. See DOI: 10.1039/b000000x

1) G. R. -Gomez, J. D. A. Tyndall, B. Pfeiffer, G. Abbenante and D. P. Fairlie, *Chem. Rev.*, 2010, **110**, PR1.
2) D. J. Craik, D. P. Fairlie, S. Liras and D. Price, *Chem. Biol. Drug. Des.*, 2013, **81**, 136.
3) For synthetic peptides based on sulfonamide linkage, see: (a) C. Gennari, B. Salom, D. Potenza, C. Longari, E. Fioravanzo, O. Carugo, and N. Sardone, *Chem. -Eur. J.*, 1996, **2**, 644; (b) J. M. Langenhan, J. D. Fisk, and S. H. Gellman, *Org. Lett.*, 2001, **3**, 2559; (c) R. M. J. Liskamp, D. T. S. Rijkers, J. A. W. Kruijtzer, J. Kemmink, *ChemBioChem.*, 2011, **12**, 1626; (d) S. Turcotte, S. H. B.-Gervais, and W. D. Lubell, *Org. Lett.*, 2012, **14**, 1318.
4) (a) K. N. Vijayadas, H. C. Davis, A. S. Kotmale, R. L. Gawade, V. G. Puranik, P. R. Rajamohanan and G. J. Sanjayan, *Chem. Commun.*, 2012, **48**, 9747.
5) (a) S. S. Kale, G. Priya, A. S. Kotmale, R. L. Gawade, V. G. Puranik, P. R. Rajamohanan and G. J. Sanjayan, *Chem. Commun.*, 2013, **49**, 2222; (b) V. V. E. Ramesh, S. S. Kale, A. S. Kotmale, R. L. Gawade, V. G. Puranik, P. R. Rajamohanan and G. J. Sanjayan, *Org. Lett.*, 2013, **15**, 1504; (c) S. S. Kale, S. M. Kunjir, R. L. Gawade, V. G. Puranik, P. R. Rajamohanan and G. J. Sanjayan, *Chem. Commun.*, 2014, **50**, 2886.
6) (a) H. N. Hoang, R. W. Driver, R. L. Beyer, A. K. Malde, G. T. Le, G. Abbenante, A. E. Mark and D. P. Fairlie, *Angew. Chem., Int. Ed.*, 2011, **50**, 11107; (b) D. Srinivas, K. N. Vijayadas, R. Gonnade, U. D. Phalgune, P. R. Rajamohanan and G. J. Sanjayan, *Org. Biomol. Chem.*, 2011, **9**, 5762.
7) (a) F. Formaggio, A. Bettio, V. Moretto, M. Crismo, C. Toniolo and Q. B. Broxterman, *J. Pept. Sci.*, 2003, **9**, 461; (b) J. Venkatraman, S. C. Shankaramma and P. Balaram, *Chem. Rev.*, 2001, **101**, 3131.
8) The C-S-N-C dihedral angle 'ω' for sulfonamide bond is ≤ 140°, A. Parkin, A. Collins, C. J. Gilmore, C. C. Wilson, *Acta Crystallogr., Sect. B*, 2008, **64**, 66.
9) D. Yang, W. Li, J. Qu, S. –W. Luo and Y. –D. Wu, *J. Am. Chem. Soc.*, 2003, **125**, 13018.
10) J. Chattergee, C. Gilon, A. Hoffman and H. Kessler, *Acc. Chem. Res.*, 2008, **41**, 1331.
11) For selected examples of backbone modification of peptides, see: (a) T. Hjelmgaard, O. Roy, L. Nauton, M. El-Ghozzi, D. Avignant, C. Didierjean, C. Taillefumier and S. Faure, *Chem. Commun.*, 2014, **50**, 3564; (b) C. Tomasini, N. Castellucci, *Chem. Soc. Rev.*, 2013, **42**, 156; (c) R. V. Nair, S. Kheria, S. Rayavarapu, A. S. Kotmale, B. Jagadeesh, R. G. Gonnade, V. G. Puranik, P. R. Rajamohanan and G. J. Sanjayan, *J. Am. Chem. Soc.*, 2013, **135**, 11477; (d) B. J. Ayers, A. F. G. Glawar, R. F. Martínez, N. Ngo, Z. Liu, G. W. J. Fleet, T. D. Butters, R. J. Nash, C.-Y. Yu, M. R. Wormald, S. Nakagawa, I. Adachi, A. Kato, and S. F. Jenkinson, *J. Org. Chem.*, 2014, **79**, 3398; (e) I. M. Mandity, A. Monsignori, L. Fulop, E. Forro, F. Fülöp, *Chem. Eur J.*, 2014, 20, 4591; (f) N. Pendem, Y. R. Nelli, C. Douat, L. Fischer, M. Laguerre, E. Ennifar, B. Kauffmann and G. Guichard, *Angew. Chem. Int. Ed.*, 2013, **52**, 4147; (g) J. Buratto, C. Colombo, M. Stupfel, S. J. Dawson, C. Dolain, B. L. d'Estaintot, L. Fischer, T. Granier, M. Laguerre, B. Gallois, I. Huc, *Angew. Chem. Int. Ed.* 2014, **53**, 883; (h) H. Lingard, J. T. Han, A. L. Thompson, I. K. H. Leung, R. T. W. Scott, S. Thompson, and A. D. Hamilton, *Angew. Chem., Int. Ed.*, 2014, **53**, 3650; (i) R. V. Nair, S. B. Baravkar, T. S. Ingole, G. J. Sanjayan, *Chem. Commun.*, 2014, **50**, 13874; (j) R. V. Nair, K. N. Vijayadas, A. Roy, G. J. Sanjayan, *Eur. J. Org. Chem.*, 2014, DOI: 10.1002/ejoc.201402877, and cited references therein.
12) CCDC no: of **1-7** are CCDC 1027031-1027037, respectively.